(s, CH_3O), 52.25 (s, CH_3O), 61.01 (d, J_{PC} = 5.6 Hz, CH_{ring}), 64.19 (d, J_{PC} = 13.0 Hz, NCH_{ring}), 148.56 (d, J_{PC} = 8.3 Hz, C=N), 169.62 (s, CO), 171.77 (s, CO); ^1H NMR ($CDCl_3$) 1.06 (m, 21 H, i-Pr_3Si), 1.33 (m, J_{HH} = 7.0 Hz, 24 H, CH_3), 3.69 (s, CH_3O, 3 H), 3.71 (s, CH_3O, 3 H), 3.77 (d, J_{HH} = 5.6 Hz, 1 H, CH_{ring}), 4.15 (sept d, J_{PH} = 15.7 Hz, J_{HH} = 7.0 Hz, 4 H, NCH), 5.10 (dd, J_{PH} = 2.0 Hz, J_{HH} = 5.6 Hz, 1 H, CH_{ring}); IR (THF) 1737 cm^{-1} (CO).

Synthesis of Oxadiazole 23. A THF solution (10 mL) of **21** (0.33 g, 0.95 mmol) was added dropwise to trimethylacetyl chloride (0.12 g, 0.95 mmol) in THF (5 mL). After the solution was stirred for 1 h at 40 °C, the solvent was removed under vacuum, and **23** was isolated by column chromatography (hexane/Et_2O, 80/20, R_f = 0.44) as a pale yellow oil (0.09 g, 34%): ^{13}C NMR ($CDCl_3$) 12.1 (s, $CHCH_3$), 17.51 (s, $CHCH_3$), 26.39 (CCH_3), 31.99 (s, CCH_3), 167.91 (s, C=N), 175.95 (s, C=N); ^1H NMR ($CDCl_3$) 1.09-1.28 (s, 21 H, i-Pr), 1.39 (s, 9 H, CCH_3); IR (THF) 1561 cm^{-1} (C=N); mass spectrum, m/e 283 (M + 1). Anal. Calcd for $C_{15}H_{30}N_2OSi$: C, 63.77; H, 10.70; N, 9.91. Found: C, 64.15; H, 10.19; N, 9.78.

Reaction of 21 with Methanol. To a THF solution (10 mL) of **21** (0.31 g, 0.84 mmol) was added an excess of methanol (0.5 mL). After evaporation of the solvent, **24** was obtained by distillation as a yellow liquid (0.16 g, 95%): bp 90-100 °C (5×10^{-2} mmHg). Its spectroscopic data were compared to those of an authentic sample.[1g]

Oxadiazole 26 was obtained by column chromatography (hexane/Et_2O, 85/15, R_f = 0.52) as a white solid (0.18 g, 57%): mp 94 °C; ^{13}C NMR ($CDCl_3$) 26.30 (s, CH_3), 27.94 (s, CH_3), 32.48 (s, CCH_3), 44.36 (s, $C(O)CCH_3$), 159.50 (C=N), 174.2 (C=N), 192.56 (CO); ^1H NMR ($CDCl_3$) 1.43 (s, 9 H, CH_3), 1.45 (s, 9 H, CH_3); IR (THF) 1702 cm^{-1} (CO), 1546 cm^{-1} (C=N); mass spectrum, m/e 211 (M + 1). Anal. Calcd for $C_{11}H_{18}N_2O_2$: C, 62.83; H, 8.63; N, 13.32. Found: C, 63.09; H, 8.72; N, 13.22.

Acetyl(trimethylstannyl)diazomethane (27) was obtained by distillation as a yellow liquid (0.33 g, 90%): bp 40 °C (5×10^{-2} mmHg). In solution, **27** was stable for weeks, but decomposed when pure: ^{13}C NMR ($CDCl_3$) -8.0 (s, $J_{C^{117}Sn}$ = 365.6 Hz, $J_{C^{119}Sn}$ = 379.2 Hz, $SnCH_3$), 25.9 (s, CH_3), 196.5 (s, CO), the CN_2 carbon atom was not observed; ^1H NMR ($CDCl_3$) 0.37 (s, $J_{H^{117}Sn}$ = 55.8 Hz, $J_{H^{119}Sn}$ = 58.1 Hz, 9 H, $SnCH_3$), 2.24 (s, 3 H, CH_3); ^{119}Sn NMR ($CDCl_3$) +25.6; ^{14}N NMR (C_6D_6) -130.8 ($\nu_{1/2}$ = 85 Hz, CNN) -49.1 ($\nu_{1/2}$ = 770 Hz, CNN); IR (THF) 2053 cm^{-1} (CN_2), 1615 cm^{-1} (CO).

Electrochemical Kinetic Discrimination of the Single-Electron-Transfer Events of a Two-Electron-Transfer Reaction: Cyclic Voltammetry of the Reduction of the Bis(hexamethylbenzene)ruthenium Dication

David T. Pierce and William E. Geiger*

Contribution from the Department of Chemistry, University of Vermont, Burlington, Vermont 05405. *Received October 10, 1991. Revised Manuscript Received April 6, 1992*

Abstract: The electrochemical reduction of $[(\eta^6\text{-}C_6Me_6)_2Ru][BF_4]_2$ has been shown to occur in two one-electron steps, each manifesting solvent-dependent formal potentials. The heterogeneous charge-transfer kinetics varied with electrode material. Cyclic voltammetry (CV) was found to be sensitive to homogeneous reactions which occurred both within the electrode reaction layer and in the bulk of solution. Whereas the reduction waves of $(C_6Me_6)_2Ru^{2+/+/0}$ were resolved in CH_2Cl_2 and separated by -0.14 V ($E^\circ_2 - E^\circ_1$, E°_2 = -1.45 V vs Fc/Fc^+), only a single two-electron wave was observed in CH_3CN because of a negative shift of E°_1 with respect to E°_2 ($E^\circ_2 - E^\circ_1$ = +0.03 V, E°_2 = -1.40 V). Both reductions displayed Nernstian behavior at Hg electrodes. However, the Ru(I/0) couple showed quasireversible charge-transfer kinetics at Pt disk electrodes. At Pt, the two-electron wave was found to split into its one-electron components over a range of sweep rates which varied with analyte concentration. The Ru(I) complex was also subject to a follow-up reaction having a rate constant of 1.0 s^{-1}. Detailed explicit finite difference simulations of the CV curves allowed solution of the electron-transfer parameters for the two one-electron couples in CH_3CN at Pt. The average values from 15 simulations over a scan rate range of 0.4-100 V s^{-1} and a concentration range of 0.50-1.3 mM were as follows: Ru(II/I), E°_1 = -1.43 V, $k_{s1} \geq 2$ cm s^{-1}; Ru(I/0), E°_2 = -1.40 V, $k_{s2} = 4.5 \times 10^{-4}$ cm s^{-1}, α_{o2} = 0.50, $d\alpha_2/dE$ = 0.22 V^{-1}. The equilibrium constant and rate constant for the disproportionation reaction 2Ru(I) $\rightleftharpoons$ Ru(II) + Ru(0) were 2.0 and 6.3×10^4 M^{-1} s^{-1}, respectively. The diffusion coefficient of the Ru(II) complex was only about 0.45 times that of the Ru(0) complex. This redox system obeyed an $E_{rev}E_{qrev}$ model down to experiment times of 10 μs. This is believed to be the first recognized example of kinetic discrimination between one-electron processes of a two-electron EE wave.

Introduction

Multielectron-transfer reactions which proceed without detectable concentrations of one-electron intermediates are important in a variety of synthetic, catalytic, and biological contexts.[1-5] Although there exists relatively limited knowledge of the mechanisms of these complex reactions,[6] electrochemistry can provide some information.[7,8] For example, well-known criteria allow diagnosis of two-electron processes in which each one-electron transfer[9,10] is Nernstian. When $E^\circ_2 \gg E^\circ_1$ (eqs 1 and 2), the couple

(1) (a) *Metal Ion Activation of Dioxygen*; Spiro, T. G. Ed.; Wiley: New York, 1980. (b) Lowe, D. J.; Fisher, K.; Thomeley, R. N. F.; Vaughn, S.; Burgess, B. K. *Biochemistry* **1989**, *28*, 8460. Seven additional references are in supplementary material.

(2) (a) Marshall, J. L.; Stobart, S. R.; Gray, H. B. *J. Am. Chem. Soc.* **1984**, *106*, 3027. (b) Rodman, G. S.; Mann, K. R. *Inorg. Chem.* **1985**, *24*, 3507. (c) Edwin, J.; Rheingold, A. L.; Geiger, W. E. *J. Am. Chem. Soc.* **1984**, *106*, 3052. Eight references are in supplementary material.

(3) (a) Kuwabata, S.; Tanaka, K.; Tanaka, T. *Inorg. Chem.* **1986**, *25*, 1691. (b) Smith, D. A.; Zhuang, B.; Newton, W. E.; McDonald, J. W.; Schultz, F. A. *Inorg. Chem.* **1987**, *26*, 2524. Five additional references are in supplementary material.

(4) (a) Evans, D. H.; Xie, N. *J. Am. Chem. Soc.* **1983**, *105*, 315. (b) Ahlberg, A.; Hammerich, O.; Parker, V. D. *J. Am. Chem. Soc.* **1983**, *105*, 844. (c) Bard, *Pure Appl. Chem.* **1971**, *25*, 379. Nine additional references are in supplementary material.

(5) (a) Fernandes, J. B.; Zhang, L. Q.; Schultz, F. A. *J. Electroanal. Chem.* **1991**, *297*, 145. Four additional references are in supplementary material.

(6) Rhodes, M. R.; Barley, M. H.; Meyer, T. J. *Inorg. Chem.* **1991**, *30*, 629. Fifteen additional references are in supplementary material.

(7) Bard, A. J.; Faulkner, L. R. *Electrochemical Methods*; John Wiley: New York, 1980; pp 111-112 contains leading references.

(8) See, also: (a) Hurd, R. M. *J. Electrochem. Soc.* **1962**, *109*, 327. (b) Marcus, R. A. *J. Phys. Chem.* **1963**, *67*, 853. (c) Reynolds, W. L.; Lumry, R. *Mechanisms of Electron Transfer*; Ronald Press: New York, 1966; pp 96-97. (d) Schwarz, H. A.; Comstock, D.; Yandell, J. K.; Dodson, R. W. *J. Phys. Chem.* **1974**, *78*, 488. (e) Mohilner, D. M. *J. Phys. Chem.* **1964**, *68*, 623. (f) Ruzic, I. *J. Electroanal. Chem.* **1974**, *52*, 331. (g) Heinze, J. *Angew. Chem., Int. Ed. Engl.* **1984**, *23*, 831.

0002-7863/92/1514-6063$03.00/0

$M^z + 2e^- \rightarrow M^{z-2}$ exhibits a single cyclic voltammetric wave with $E_{pa} - E_{pc} = 28.5$ mV at a formal potential $E^\circ(app) = (E^\circ_2 + E^\circ_1)/2$.[11] No direct information about the one-electron intermediate M^{z-1} is realized from this measurement alone.

$$M^z + e^- \rightleftharpoons M^{z-1} \qquad E^\circ_1 \qquad (1)$$

$$M^{z-1} + e^- \rightleftharpoons M^{z-2} \qquad E^\circ_2 \qquad (2)$$

Knowledge about the individual one-electron steps of a composite two-electron wave can sometimes be acquired if alteration of solvent, pH, or counterions results in preferential stabilization of one electron-transfer (et) reaction and separation of the $2e^-$ wave into two $1e^-$ processes.[12] One thereby attains *thermodynamic discrimination* between the two et reactions.

Kinetic discrimination between the electron-transfer reactions is also possible, in principle, if one reaction is impeded by a slow heterogeneous charge transfer. If the second electron transfer is considerably slower than the first, the contribution of the cathodic process of eq 2 to the overall reaction depends on both the applied potential and the experimental observation time.[11,13-15] Owing to the latter, the shapes of CV curves for non-Nernstian EE systems with $E^\circ_2 > E^\circ_1$ are scan rate dependent. In the slow scan limit, a single two-electron wave is observed;[11,27] in the fast scan limit, two one-electron waves would be present, each behaving as independent entities, with characteristics typical of the individual one-electron reactions.[16] One expects that chemical systems with a small value of ΔE° ($= E^\circ_2 - E^\circ_1$) would have the most readily observable kinetic discrimination effect, since this circumstance minimizes the potential shifts (and thereby, changes in scan rate) required to view splitting of the single two-electron wave into two one-electron waves.[17]

Though recognized as a theoretical concept,[15,18,19] kinetic discrimination in the voltammetry of multielectron waves had apparently not been reported until the present work.[20] Several factors led us to study the reduction of the symmetric π complex $(\eta^6\text{-}C_6Me_6)_2Ru^{2+}$, $\mathbf{1}^{2+}$, in searching for experimental verification of kinetic discrimination. This ion is known to reduce by two electrons to a neutral complex with a bent arene.[21] The E° separation between the reactions of eqs 3 and 4 is known to be small and solvent dependent.[22] The hapticity change is likely to occur in the *second* reduction (eq 4), thereby making the second

$$(\eta^6,\eta'^6\text{-}C_6Me_6)_2Ru^{2+} + e^- \rightleftharpoons (\eta^6,\eta'^6\text{-}C_6Me_6)_2Ru^{+} \qquad Ru(II)/Ru(I) \quad (3)$$

$$(\eta^6,\eta'^6\text{-}C_6Me_6)_2Ru^{+} + e^- \rightleftharpoons (\eta^6,\eta'^4\text{-}C_6Me_6)_2Ru^{0} \qquad Ru(I)/Ru(0) \quad (4)$$

et reaction inherently slower than the first.[23,24] Furthermore, et reactions involving arene hapticity changes have been shown to be particularly slow at Pt electrodes in CH_3CN,[25] possibly enhancing the difference between the rates of the heterogeneous charge transfer processes for eqs 3 and 4. Finally, earlier voltammetry reported on this complex indicated qualitatively unusual responses at high sweep rates.[22] In this paper we show that increases in CV sweep rates change this redox couple from one showing an essentially Nernstian $2e^-$ single wave to one in which the two one-electron waves are clearly resolved, each wave having voltammetric characteristics arising only from its own one-electron reaction. A preliminary communication of this work has appeared.[26]

It is important to note that the above remarks concerning historical precedents for kinetic discrimination are made purely within the context of EE mechanisms.[27] Other potentially time-dependent mechanisms (e.g., CEE, ECE, and EEC), in which reactions such as isomerizations occur separately from the et step, are only germane for comparison purposes.[28-43] We justify treatment of the $(C_6Me_6)_2Ru^{2+/+/0}$ reduction as an EE process in the beginning of the Results section.

The redox chemistry of $(\eta^6\text{-}C_6Me_6)_2Ru^{2+}$ is quite interesting in its own right. Elschenbroich treated this ion with sodium to synthesize the first deliberately prepared bent (tetrahapto) arene complex,[21] $(\eta^6\text{-}C_6Me_6)(\eta^4\text{-}C_6Me_6)Ru$, **2**, over two decades ago. Voltammetry on $\mathbf{1}^{2+}$ and related complexes later revealed a single two-electron wave of limited chemical reversibility in CH_3CN[22a] and two barely resolved one-electron waves in CH_2Cl_2.[22b] A series of papers by Finke, Boekelheide, and co-workers elegantly addressed the effect of geometric rigidity of the arene (e.g., in cyclophane derivatives) on the redox properties.[22,44] Two-electron

(9) This discussion assumes that multielectron transfers occur in discrete one-electron steps. For one viewpoint of this assumption, see: Richardson, D. E.; Taube, H. *Coord. Chem. Rev.* **1984**, *60*, 107, especially p 125ff.

(10) This assumption becomes more debatable when considering inner-sphere processes: (a) Gurnee, E. F.; Magee, J. L. *J. Chem. Phys.* **1957**, *26*, 1237. (b) Taube, H. In *Mechanistic Aspects of Inorganic Reactions, ACS Symposium Series, 198*; Rorabacher, D. B., Endicott, J. F., Eds.; Washington, DC, Chapter 7. (c) Zhen, Y.; Feighery, W. G.; Lai, C.-K.; Atwood, J. D. *J. Am. Chem. Soc.* **1989**, *111*, 7832.

(11) Polcyn, D. S.; Shain, I. *Anal. Chem.* **1966**, *38*, 370.

(12) (a) Boyd, D. C.; Rodman, G. S.; Mann, K. R. *J. Am. Chem. Soc.* **1986**, *108*, 1779. (b) Smith, W. H.; Bard, A. J. *J. Electroanal. Chem.* **1977**, *76*, 19. (c) Laviron, E. *J. Electroanal. Chem.* **1983**, *148*, 1. Nine additional references are in supplementary material.

(13) The dependence on experiment time is an implicit characteristic of quasireversible and irreversible redox (E) systems (see ref 7, p 109). For EE systems, see refs 14 and 15.

(14) Ryan, M. D. *J. Electrochem. Soc.* **1978**, *125*, 547.

(15) Hinkelmann, K.; Heinze, J. *Ber. Bunsenges Phys. Chem.* **1987**, *91*, 243.

(16) This limit reduces to the $E_{rev}E_{irrev}$ case of ref 11.

(17) There has been considerable theoretical treatment of EE systems with $\Delta E^\circ = 0$: (a) Reference 8g, 11, and 12*f*. (b) Myers, R. L.; Shain, I. *Anal. Chem.* **1969**, *41*, 980. (c) Richardson, D. E.; Taube, H. *Inorg. Chem.* **1981**, *20*, 1278.

(18) (a) Tsaur, K.-C.; Pollard, R. *J. Electroanal. Chem.* **1985**, *183*, 91 (differential pulse polarography). (b) Galvez, J.; Park, S.-M. *J. Electroanal. Chem.* **1987**, *235*, 71 (pulse polarography).

(19) Grzeszczuk, M.; Smith, D. E. *J. Electroanal. Chem.* **1984**, *162*, 189 (ac polarography, wave broadening but not splitting predicted).

(20) Chronoamperometric measurements on the reduction of TcO_4^- in basic media show a dependence on gelatin concentration which has been interpreted in terms of preferential lowering of the kinetics of the $TcO_4^{2-/3-}$ couple: Kissel, G.; Feldberg, S. W. *J. Phys. Chem.* **1969**, *73*, 3082.

(21) Fischer, E. O.; Elschenbroich, C. *Chem. Ber.* **1970**, *103*, 162.

(22) (a) Laganis, E. D.; Voegeli, R. H.; Swann, R. T.; Finke, R. G.; Hopf, H.; Boekelheide, V. *Organometallics* **1982**, *1*, 1415. (b) Finke, R. G.; Voegeli, R. H.; Langanis, E. D.; Boekelheide, V. *Organometallics* **1983**, *2*, 347.

(23) Merkert, J.; Nielson, R. M.; Weaver, M.; Geiger, W. E. *J. Am. Chem. Soc.* **1989**, *111*, 7084.

(24) Marcus, R. A. *Ann. Rev. Phys. Chem.* **1964**, *15*, 155.

(25) Bowyer, W. J.; Geiger, W. E. *J. Electroanal. Chem.* **1988**, *239*, 253.

(26) Pierce, D. T.; Geiger, W. E. *J. Am. Chem. Soc.* **1989**, *111*, 7636.

(27) We employ the usual symbols of E for a heterogeneous electron transfer and C for a chemical reaction.

(28) Heinze, J.; Dietrich, M.; Hinkelmann, K.; Meerholz, K.; Rashwan, F. *Dechema-Monogr.* **1989**, *112*, 61 and references therein.

(29) Crooks, R. M.; Bard, A. J. *J. Electroanal. Chem.* **1988**, *243*, 117.

(30) Laviron, E. *J. Electroanal. Chem.* **1986**, *208*, 357.

(31) Deakin, M. R.; Wightman, R. M. *J. Electroanal. Chem.* **1986**, *206*, 167.

(32) Dietrich, M.; Heinze, J.; Fischer, H.; Neugebauer, F. A. *Angew. Chem., Int. Ed. Engl.* **1986**, *25*, 1021.

(33) Gaudiello, J. G.; Wright, T. C.; Jones, R. A.; Bard, A. J. *J. Am. Chem. Soc.* **1985**, *107*, 888.

(34) Moulton, R.; Weidman, T. W.; Vollhardt, K. P. C.; Bard, A. J. *Inorg. Chem.* **1986**, *25*, 1846.

(35) Kuchynka, D. J.; Kochi, J. K. *Inorg. Chem.* **1988**, *27*, 2574; **1989**, *28*, 855.

(36) Hinkelmann, K.; Heinze, J.; Schacht, H.-T.; Field, J. S.; Vahrenkamp, H. *J. Am. Chem. Soc.* **1989**, *111*, 5078.

(37) Martone, D. P.; Osvath, P.; Lappin, A. G. *Inorg. Chem.* **1987**, *26*, 3094.

(38) Olsen, B. A.; Evans, D. H. *J. Am. Chem. Soc.* **1981**, *103*, 839.

(39) Hammerich, O.; Parker, V. D. *Acta Chem. Scand.* **1981**, *B35*, 395.

(40) (a) Evans, D. H.; Busch, R. W. *J. Am. Chem. Soc.* **1982**, *104*, 5057. (b) Evans, D. H.; Xie, N. *J. Electroanal. Chem.* **1982**, *133*, 367.

(41) Wave splitting has been reported in two recent papers lacking detailed mechanistic analysis: (a) deLearie, L. A.; Pierpont, C. G. *J. Am. Chem. Soc.* **1987**, *109*, 7031. (b) Drake, S. R.; Barley, M. H.; Johnson, B. F. G.; Lewis, J. *Organometallics* **1988**, *7*, 806.

(42) Edwin, J.; Geiger, W. E. *J. Am. Chem. Soc.* **1990**, *112*, 7104.

(43) Geiger, W. E.; Salzer, A.; Edwin, J.; von Philipsborn, W.; Piantini, U.; Rheingold, A. L. *J. Am. Chem. Soc.* **1990**, *112*, 7113.

couples are extremely rare for metal sandwich complexes.[45]

Studies on isoelectronic rhodium (η^6-arene)$RhCp^{*2+}$ complexes,[23,46-48] in which the one-electron intermediate in the sequence (arene)$RhCp^{*2+/+/0}$ is thermodynamically stable, are pertinent because they suggest strongly that the arene bends in the *second* of the two one-electron transfer reactions. This provides the justification for writing the structures below in the Ru(II)/Ru(I)/Ru(0) reaction sequence.

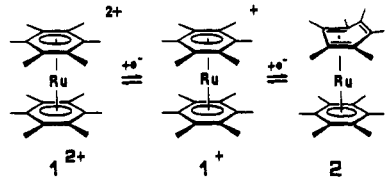

A recent theoretical discussion is pertinent in which Richardson and Taube relate kinetic factors, specifically the time delay between successive $1e^-$ transfers, to changes between a $2e^-$ process and two $1e^-$ processes.[9] The present observation of kinetic discrimination in the et reactions of $(C_6Me_6)_2Ru^{2+/+/0}$ is related conceptually to their ideas.

Experimental Section

Electrochemistry. Solvents for electrochemical experiments were dried and deoxygenated before use. Dichloromethane (HPLC grade, Aldrich or Baker) was distilled from CaH_2. Acetonitrile and dimethylformamide (DMF) were free of detectable electrochemical impurities as received from Burdick and Jackson, requiring only drying over molecular sieve (type 4A, Linde) before use. Standard methods for solvent deoxygenation were followed, usually involving three freeze–pump–thaw cycles. The supporting electrolyte was tetra-*n*-butylammonium hexafluorophosphate, Bu_4NPF_6, normally 0.1 M.

Experiments at subambient temperatures (±1°) and bulk electrolyses and rotating disk electrode voltammetry were carried out in a VAC drybox with the electrolysis cell partially immersed in a thermostated heptane bath. CV experiments on the benchtop utilized a greaseless sealed cell. Prepurified nitrogen was passed through silica gel, copper deoxygenation catalyst, and solvent. Potential control was maintained with PARC instrumentation (Models 173, 179, and 175 potentiostat and peripheral gear) except when scan rates above 200 V s^{-1} were necessary. In those cases, an EI-350 potentiostat (Ensman Instrumentation, Bloomington, IN) constructed for fast response at ultramicroelectrodes was used with the cell and preamplifiers isolated inside a grounded Faraday cage. Hydrodynamic control at a rotating Pt disk electrode was provided by a Pine Instruments (Grove City, PA) ASR2 synchronous rotator (500–3000 rpm). A Sargent-Welch rotator (S-76485, 1800 rpm) served the same purpose in experiments employing a rotating Pt bead electrode.

CV scans utilized homemade Pt bead or Kemula-type hanging Hg drop electrodes as well as Pt disks of 500-, 238-, 100-, or 10-μm diameter. The area of the rotating Pt disk electrode (Pine Instruments) was measured as 0.591 ± 0.003 cm^2 from the Cottrell equation using $[K_4][Fe(CN)_6]$ in aqueous 2.0 M KCl. The larger working electrodes were pretreated by polishing with 0.25 μm diamond paste, and electrodes with $d < 100$ μm were polished with 0.05 μm alumina on microcloth (Buehler, Ltd.). A three-electrode configuration was used, with the functional reference electrode being Ag/AgCl. However, the reference redox couple in this paper is ferrocene(Fc)/ferrocenium.[49] Fc was added to the cell at the end of each experiment. If desired, the reported potentials may be referenced to the popular aqueous SCE scale by addition of +0.40 V (CH_3CN) or +0.46 V (CH_2Cl_2) to the reported potentials.

Voltammetric waveforms at scan rates, v, below 0.5 V s^{-1} were recorded on a Hewlett-Packard XY recorder (7046B). All other data were acquired and stored on a Nicolet 4094A digital oscilloscope equipped with a no. 4175 8-bit plug in (minimum 5 ns sampling time) and F-43/2 dual disk recorder. Signal averaging of 5–20 CV scans improved the voltammetric displays. Further data processing was accomplished with a Swan XT10 personal computer.

Scheme I

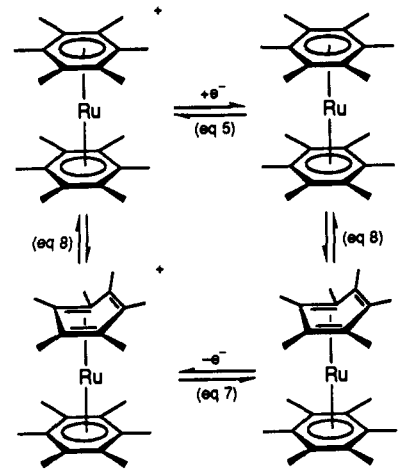

Voltammetric distortions owing to solution resistance were minimized by use of the smallest working electrode consistent with introduction of <3% radial diffusion[50] and by employment of positive feedback compensation in PARC 173 experiments. Efficient compensation was achieved by shunting a second Pt wire to the reference electrode with a 0.1 μF capacitor.[51] Evaluation of fast redox couples adequately reproduced literature data.[52] Charging current subtraction was employed in high sweep rate CV experiments by recording matching waveforms before and after additions of analyte, followed by point-by-point subtraction and smoothing using a polynomial smoothing routine. Explicit finite difference simulations of CV's as described by Feldberg[53] were executed on the XT10 using a Microsoft FORTRAN Optimizing Compiler (version 4.1, Microsoft, Redmond, WA) or on a VAX 8600 (Digital Equipment) available through the University of Vermont.

Compounds. Compounds $(\eta^6\text{-}C_6Me_6)_2Ru^{2+}$, $\mathbf{1}^{2+}$, and $(\eta^6\text{-}C_6Me_6)(\eta^4\text{-}C_6Me_6)Ru$, **2**, were prepared by literature methods[54] using standard Schlenck procedures and carefully purified solvents. Their purities were checked by NMR and by elemental analysis (C, H: Robertson Laboratories). $\mathbf{1}^{2+}$ was recrystallized as the tetrafluoroborate salt from nitromethane/diethyl ether (vapor) and dried in vacuo, yielding a white microcrystalline powder. **2** was obtained as long prismatic orange crystals by slow cooling of its hexane solutions to 243 K.

Results

Mechanistic Overview: Grounds for EE Treatment. We show below that the $(C_6Me_6)_2Ru^{2+/+/0}$ redox system, $\mathbf{1}^{2+}/\mathbf{1}^{+}/\mathbf{2}$,[55] is adequately treated with an $E_{rev}E_{qrev}$ mechanism. Over a factor of nearly 10^6 range in scan rates the second reduction goes from nearly Nernstian to completely irreversible in its voltammetric response. Redox reactions involving significant structural changes must take account of the relative timing of the electron-transfer

(44) Plitzko, K-D.; Wehrle, G.; Gollas, B.; Rapko, B.; Dannheim, J.; Boekelheide, V. *J. Am. Chem. Soc.* **1990**, *112*, 6556. Five additional references are in supplementary material.

(45) Geiger, W. E. In *Organometallic Radical Processes*; Trogler, W. C., Ed.; Elsevier: Amsterdam, 1990; p 142ff.

(46) Bowyer, W. J.; Geiger, W. E. *J. Am. Chem. Soc.* **1985**, *107*, 5657.

(47) Bowyer, W. J.; Merkert, J. W.; Geiger, W. E.; Rheingold, A. L. *Organometallics* **1989**, *8*, 191.

(48) Nielson, R. M.; Weaver, M. J. *Organometallics* **1989**, *8*, 1636.

(49) Gritzner, G.; Kuta, J. *Pure Appl. Chem.* **1984**, *56*, 461.

(50) (a) Heinze, J. *Ber. Bunsenges. Phys. Chem.* **1981**, *85*, 1096. (b) Bowyer, W. J.; Engelmann, E. E.; Evans, D. H. *J. Electroanal. Chem.* **1989**, *262*, 67.

(51) Garreau, D.; Saveant, J. M.; Binh, S. K. *J. Electroanal. Chem.* **1978**, *89*, 427.

(52) A standard heterogeneous electron-transfer rate, k_s, of 2 cm s^{-1} was measured for Fc/Fc^+ in CH_3CN at Pt disks, close to the apparent best literature value of 3 cm s^{-1} see: (a) Wipf, D. O.; Kristensen, E. W.; Deakin, M. R.; Wightman, R. M. *Anal. Chem.* **1988**, *60*, 306. (b) Gennett, T.; Milner, D. F.; Weaver, M. J. *J. Phys. Chem.* **1985**, *89*, 2787. (c) Gennett, T.; Weaver, M. J. *J. Electroanal. Chem.* **1985**, *186*, 179. [See, however, recent measurements at nanometer-sized electrodes which suggest a much higher k_s value for Fc/Fc^+: Penner, R. M.; Heben, M. J.; Longin, T. L.; Lewis, N. S. *Science* **1990**, *250*, 1118. Pendley, B. D.; Abruna, H. D. *Anal. Chem.* **1990**, *62*, 782.] Similar measurements on cobaltocene/cobaltocenium gave k_s = 0.90 cm s^{-1}, compared to literature values of 0.86 cm s^{-1} (Geiger, W. E.; Smith, D. E. *J. Electroanal. Chem.* **1974**, *50*, 31) and 2.0 cm s^{-1} [ref 52c] reported from ac polarography at Hg electrodes. Sample data: CV peak separations for $Cp_2Co^{0/+}$ were 58 ± 4 mV up to v = 20 V s^{-1} with a d = 476 μm Pt disk.

(53) Feldberg, S. W. In *Electroanalytical Chemistry*; Bard, A. J., Ed.; Dekker: New York, 1969; Vol. 3, p 199.

(54) (a) Bennett, M. A.; Haug, T. N.; Matheson, T. W.; Smith, A. K. *Inorg. Synth.* **1982**, *21*, 76. (b) Bennett, M. A.; Matheson, T. W. *J. Organomet. Chem.* **1979**, *175*, 87.

(55) We employ $\mathbf{1}^{n+}$ to symbolize structures which contain a hexahapto arene and $\mathbf{2}^{n+}$ to symbolize tetrahapto arene structures, of which only the neutral complex is detected.

process and the structural rearrangement.[56,57] In many cases, the et reaction and conformational change (or isomerization) have been shown to occur sequentially and may be treated with "box schemes" involving ECE- or EEC-type formulations.[56-58]

In the present setting, *sequential* treatment of the et/structural change would involve replacing eq 4 with eqs 5–8 (also depicted in Scheme I, a square scheme).

$$(\eta^6\text{-}C_6Me_6)_2Ru^+ + e^- \rightleftharpoons (\eta^6\text{-}C_6Me_6)_2Ru \quad (5)$$

$$(\eta^6\text{-}C_6Me_6)_2Ru \rightleftharpoons (\eta^6\text{-}C_6Me_6)(\eta^4\text{-}C_6Me_6)Ru \quad (6)$$

$$(\eta^6\text{-}C_6Me_6)(\eta^4\text{-}C_6Me_6)Ru - e^- \rightleftharpoons (\eta^6\text{-}C_6Me_6)(\eta^4\text{-}C_6Me_6)Ru^+ \quad (7)$$

$$(\eta^6\text{-}C_6Me_6)(\eta^4\text{-}C_6Me_6)Ru^+ \rightleftharpoons (\eta^6\text{-}C_6Me_6)_2Ru^+ \quad (8)$$

When an isomerization is very fast on the time scale of the electrochemical experiment, it may appear to be "concurrent with" electron transfer; voltammograms would obey the criteria of "one-step" et reactions.[48,56,59] As pointed out by Evans and O'Connell,[57] the existence of reactions with concurrent et and large structural rearrangement is very difficult to prove. In electrochemical language, an EE mechanism may display the same voltammetric behavior as will an EEC (fwd)/ECE(bkwd) mechanism if the C step is fast and reversible. However, unless specific evidence for structural intermediates is uncovered, it is proper to assign a mechanism as E or EE with maximum lifetimes of structural intermediates,[56] and that is the approach taken herein.

Very fast scans (up to 10^5 V s^{-1}) reveal no new features in the $1^{2+}/1^+/2$ system which could be attributed to isomers in other oxidation states, i.e., either $(\eta^6\text{-}C_6Me_6)_2Ru$, **1**, or $(\eta^6\text{-}C_6Me_6)(\eta^4\text{-}C_6Me_6)Ru^+$, 2^+. Therefore on the experimental time scale 10 $\mu s < t < 10$ s, the reduction of $(\eta^6\text{-}C_6Me_6)_2Ru^{2+}$ is properly treated as an EE mechanism through eqs 3 and 4.

Voltammetric Overview: General Behavior of $(C_6Me_6)_2Ru^{2/+/0}$, Solvents and Electrodes. As noted in earlier literature,[22] $1^{2+}/1^+/2$ displays a single two-electron wave in CH_3CN and resolved one-electron waves in CH_2Cl_2. This thermodynamic discrimination arises from unequal solvent dependence of the E^o's of the 2+/+ and +/0 couples. We found that in CH_3CN and DMF, the single wave *splits* into two cathodic and two anodic features at high sweep rates. Data in the former solvent (CH_3CN) were quantitatively treated. Wave splitting was observed at both Pt and Au electrodes.[60] Chronocoulometric Anson plots[61] for double potential step times below 1 s were linear with equal but opposite slopes, indicating the apparent absence of significant short-time adsorption. Chronoamperometric forward step currents followed a Cottrellian dependence,[62] establishing diffusion control at high overpotentials. Diffusion coefficients of 1^{2+} calculated from these results were $D_o = 6.8 \times 10^{-6}$ cm^2 s^{-1} in CH_2Cl_2 and 7.6×10^{-6} cm^2 s^{-1} in CH_3CN (Table III).

Side Reaction of 1^+. Both the dication 1^{2+} and the neutral compound **2** are indefinitely stable in the solvents employed[63] and may be studied independently. Yet, the reduction of 1^{2+} and the oxidation of **2** do not demonstrate complete *chemical* reversibility, owing apparently to reaction(s) of the intermediate monocation generated during voltammetric cathodic or anodic scans. The product of this reaction has an irreversible reduction at −2.3 V, and although it appears to involve an H-atom transfer reaction of $(\eta^6\text{-}C_6Me_6)_2Ru^+$, its identity has not yet been unequivocally established.[64] A rate constant of 1.0 ± 0.1 s^{-1} was established for the decomposition of 1^+ from CV simulations which assumed a first- or pseudo-first-order reaction. Above $v = 0.5$ V s^{-1} this side reaction was not detectable.

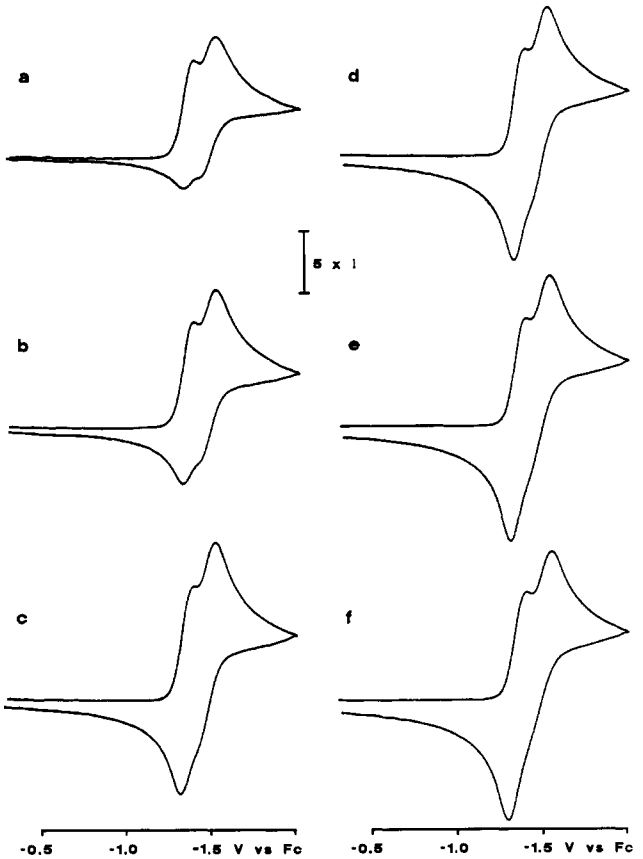

Figure 1. Slow CV scans of ca. 0.5 mM $[(\eta^6\text{-}C_6Me_6)_2Ru][BF_4]_2$ in CH_2Cl_2 at Pt disk ($d = 0.21$ cm). Scan rates: (a) 0.1, (b) 0.2, (c) 0.5, (d) 1.0, (e) 2.0, and (f) 5.0 V s^{-1}. Current axis normalized for sweep rate, $i = 1$ μA (V $s^{-1})^{-1/2}$; ohmic compensation 10 kΩ; $T = 298$ K.

Table I. Cyclic Voltammetric Data for $(\eta^6\text{-}C_6Me_6)_2Ru^{2+}$ in CH_2Cl_2 at Pt and Hg Electrodes[c]

	$(C_6Me_6)_2Ru^{2+/+}$					$(C_6Me_6)_2Ru^{+/0}$		
v (V/s^{-1})	ΔE_p (mV)	δE_p[a] (mV)	$E_{1/2}$ (V)	$i_p/v^{1/2}$ (μ$As^{1/2}$ $V^{-1/2}$)		E_{pc} (V)	ΔE_p (mV)	$E_{1/2}$ (V)
A. Pt Disk Electrode[d]								
0.10	59	65	−1.35	7.9		−1.51	94	−1.46
0.20	58	65	−1.35	8.4		−1.51	123	−1.45
0.30	62	71	−1.35	8.4		−1.52	*b*	*b*
0.40	62	65	−1.35	8.7		−1.52	*b*	*b*
0.50	62	74	−1.35	8.8		−1.53	*b*	*b*
1.0	67	71	−1.35	8.6		−1.53	*b*	*b*
B. Hg Drop Electrode[e]								
0.05	58	50	−1.36	3.8		−1.47	58	−1.44
0.10	59	52	−1.36	3.8		−1.47	59	−1.44
0.15	58	50	−1.36	3.8		−1.47	58	−1.44
0.20	58	52	−1.36	3.8		−1.47	59	−1.44
0.30	60	54	−1.36	4.0		−1.47	59	−1.44

[a] $\delta E_p = E_p - E_{p/2}$. [b] Return peak not resolved. [c] Conditions: ambient temperatures, saturated solution of $(\eta^6\text{-}C_6Me_6)_2Ru^{2+}$ (ca. 0.5 mM), potentials vs Fc/Fc^+. [d] $d = 2.08$ mm, ohmic compensation 10 kΩ. [e] Not adjusted for change in electrode area compared to Pt disk.

The $(C_6Me_6)_2Ru^{2+/+/0}$ Couples in CH_2Cl_2. CV of $(\eta^6\text{-}C_6Me_6)_2Ru^{2+}$ in CH_2Cl_2 showed two reduction waves with $E_{1/2}$[67] values of −1.35 and −1.45 V at low scan rates (Figure 1a). The first of these waves exhibited diffusion-controlled and nearly Nernstian behavior (see values of ΔE_p and $E_p - E_{p/2}$ in Table I). The second wave was quasireversible with ΔE_p values of 120–140 mV at $v = 0.2$ V s^{-1}. At higher sweep rates, peak separations of the second reduction were so large that the anodic peaks of the Ru(II/I) and Ru(I/0) processes overlapped, yielding only a single return wave. However, the cathodic and anodic contributions for

(56) Geiger, W. E. In *Progress in Inorganic Chemistry*; Lippard, S. J., Ed.; John Wiley and Sons: New York, 1985; Vol. 33, p 275.
(57) Evans, D. H.; O'Connell, K. M. In *Electroanalytical Chemistry*; Bard, A. J., Ed.; Marcel Dekker: New York, 1986; Vol. 14, p 113.
(58) (a) Bernardo, M. M.; Robandt, P. V.; Schroeder, R. R.; Rorabacher, D. B. *J. Am. Chem. Soc.* **1989**, *111*, 1224. (b) Bond, A. M.; Oldham, K. B. *J. Phys. Chem.* **1983**, *87*, 2492 and references therein.
(59) (a) Mairanovsky, V. G. *J. Electroanal. Chem.* **1981**, *125*, 231. (b) Andrieux, C. P.; Blocman, C.; Dumas-Bouchiat, J. M.; Saveant, J. M. *J. Am. Chem. Soc.* **1979**, *101*, 3431.
(60) Data at Hg electrodes was less reproducible, especially with CH_3CN as solvent.
(61) Anson, F. C.; Osteryoung, R. A. *J. Chem. Educ.* **1983**, *60*, 293.
(62) Reference 7, p 143.
(63) This was confirmed by both electrochemistry and by NMR studies in deuterated solvents.

Table II. Cyclic Voltammetric Data for $(C_6Me_6)_2Ru^{2+}$ in CH_3CN at Pt and Hg electrodes[a]

	$(C_6Me_6)_2Ru^{2+/+}$, Ru(II/I)					$(C_6Me_6)_2Ru^{+/0}$, Ru(I/O)		
v (V s^{-1})	ΔE_p (mV)	δE_p[a] (mV)	$E_{1/2}$ (V)	$i_p/v^{1/2}$ ($\mu As^{1/2}$ $V^{-1/2}$)	i_a/i_c	E_{pc} (V)	ΔE_p (mV)	$E_{1/2}$ (V)
			A. Pt Disk Electrode[e]					
0.10	88[b]	43	−1.48[b]	37.4	0.42			
0.20	116[b]	45	−1.48[b]	36.8	0.49			
0.50	194[b]	53	−1.45[b]	34.2	0.57			
			B. Pt Disk Electrode[f]					
1.0	*c*	55	*c*	0.73	*c*			
2.0	*c*	58	*c*	0.68	*c*			
5.0	68	58	−1.43	0.61	*c*	−1.63	484	−1.39
10.0	65	58	−1.42	0.56	*c*	−1.65	539	−1.38
20.0	65	58	−1.43	0.55	0.86	−1.69	598	−1.39
50.0	66	58	−1.43	0.54	0.91	−1.72	660	−1.39
100	67	58	−1.42	0.54	0.93	−1.74	706	−1.39
200	73	60	−1.43	0.53	0.98	−1.78	776	−1.39
			C. Hg Drop Electrode[g]					
0.05	42	36	−1.41	8.3	0.59			
0.10	42	36	−1.41	8.2	0.68			
0.20	42	38	−1.41	8.2	0.76			
0.50	44	40	−1.42	8.3	0.86			
1.0	45	42	−1.41	8.3	0.88			
2.0	54	44	−1.41	8.5	0.84			
5.0	61	50	−1.42	8.8	0.80			

[a] $\delta E_p = E_p - E_{p/2}$. [b] At this scan rate the wave behaves like a two-electron system. [c] Peaks for one-electron couple not resolved. [d] Conditions: ambient temperatures, potentials vs Fc/Fc^+. [e] d = 2.08 mm, ohmic compensation 2.0 kΩ, conc = 0.99 mM. [f] d = 476 μm, ohmic compensation 26 kΩ, conc = 1.31 mM. [g] Conc = 0.27 mM.[b,d]

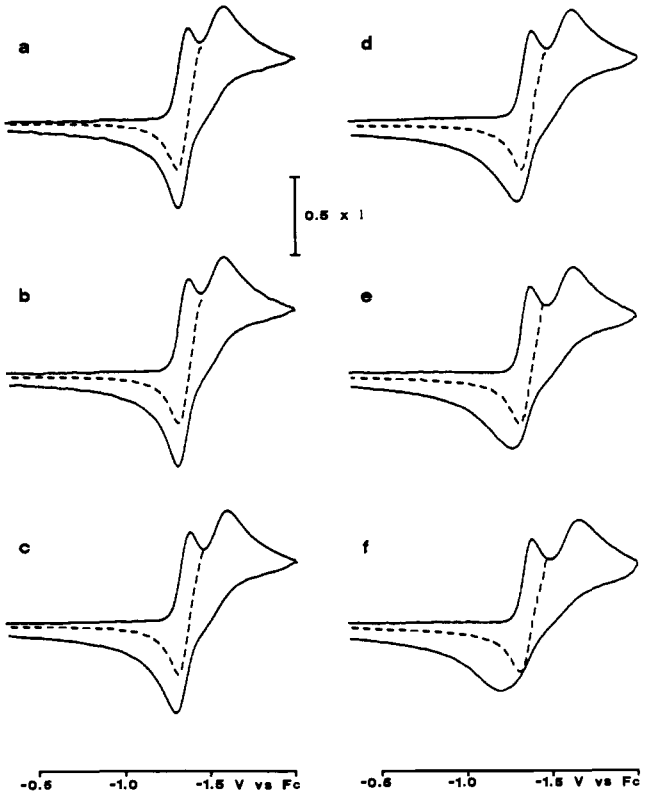

Figure 2. Faster CV scans of solution of Figure 1 (1^{2+} in CH_2Cl_2) at Pt disk (d = 476 μm). Scan rates: (a) 1.0, (b) 2.0, (c) 5.0, (d) 10, (e) 20, and (f) 50 V s^{-1}. Current axis normalized for sweep rate, i = 1 μA (V s^{-1})$^{-1/2}$; ohmic compensation 80 kΩ.

the Ru(II/I) process were directly measured by clipping of the potential scan (Figure 2, dashed lines). The presence of a slow follow-up reaction of $(C_6Me_6)_2Ru^+$ (vide ante) was diagnosed both by the diminished overall anodic currents at lower sweep rates and by the results of double potential step chronoamperometry. Bulk coulometry negative of the second wave at 253 K led to passage of only 1.0 F and replacement of the original waves with irreversible oxidation waves at E_{pa} = +0.1 and +0.4 V. The $1e^-$ coulometric conversion arises from the dominance of the decomposition reaction of the Ru(I) monocation (eq 14, vide infra) on the bulk electrolysis time scale. Although the products remain unidentified,[64] their subsequent oxidation was shown to regenerate $(C_6Me_6)_2Ru^{2+}$ in about 65% yield, without other electroactive products. The results in this solvent are important for qualitative mechanistic aspects, namely that (a) separate one-electron steps occur, (b) $k_{s2} < k_{s1}$, and (c) the one-electron Ru(I) intermediate decomposes on a longer time scale. Rough fits of experiments in the scan rate range 0.1–0.5 V s^{-1} to digital simulations[68] were found to be consistent with E°_1 = −1.32 V, E°_2 = −1.46 V, k_{s1} = fast, $k_{s2} = 4.7 \times 10^{-3}$ cm s^{-1}, α_2 = 0.50.

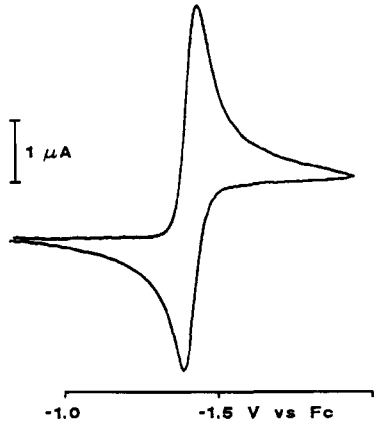

Figure 3. CV scan of 0.27 mM $[(\eta^6\text{-}C_6Me_6)_2Ru][BF_4]_2$ in CH_3CN at hanging Hg drop electrode, scan rate 0.2 V s^{-1}.

The $(C_6Me_6)_2Ru^{2+/+/0}$ Couples in CH_3CN. A. Qualitative Aspects and Assignment of Voltammetric Peaks. A single wave

(64) Pierce, D. T. Ph.D. Dissertation, University of Vermont, 1991, pp 57–67. Reactions of this type are well-established for the analogous Fe systems. For leading references, see: Astruc, D. *Chem. Rev.* **1988**, *88*, 1189.

(65) Λ_n is a dimensionless parameter equal to $k_s[D_{z-n+1}{}^{(1-\alpha)}D_{z-n}{}^{\alpha}(nFv/RT)]^{-1/2}$, n = 1, 2.

(66) The second-order rate constant k_{disp} (eq 10 or 16) is expressed in dimensionless terms as $\lambda = k_{disp}C_z(RT/nFv)$.

(67) $E_{1/2}$ values are calculated from the average of E_{pc} and E_{pa} for a couple. When the charge transfer is fast or α is 0.5, $E_{1/2}$ is very close to the formal potential $E^{o\prime}$.

(68) Digital simulations of the $(C_6Me_6)_2Ru^{2+/+/0}$ system in CH_2Cl_2 gave ambiguous fits owing to the lack of resolution of the two anodic waves and the ohmic distortions occurring at high sweep rates. See ref 64 for details.

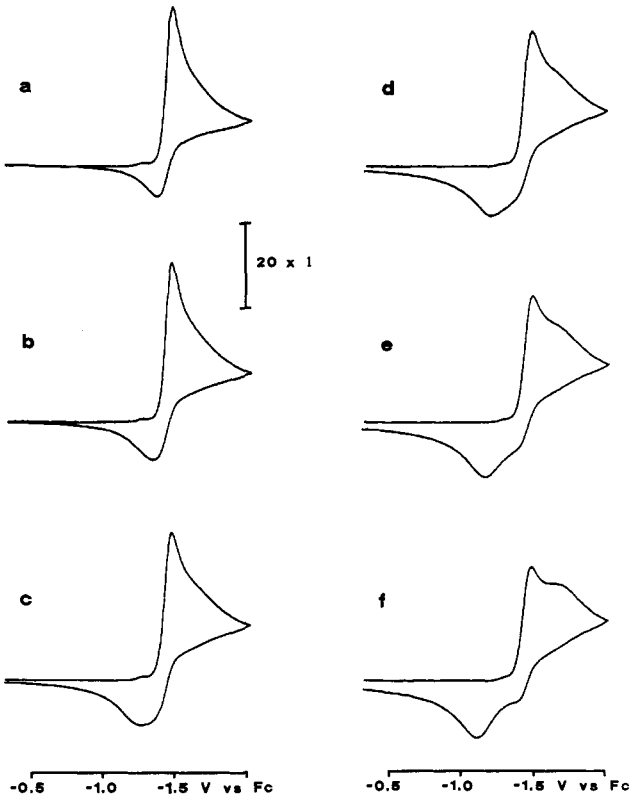

Figure 4. Slow CV scans of 1.0 mM $[(\eta^6\text{-}C_6Me_6)_2Ru][BF_4]_2$ in CH_3CN at Pt disk (d = 0.21 cm). Scan rates (a) 0.1, (b) 0.2, (c) 0.5, (d) 1.0, (e) 2.0, and (f) 5.0 V s^{-1}. Current axis normalized for sweep rate, i = 1 μA (V s^{-1})$^{-1/2}$; ohmic compensation 2.0 kΩ.

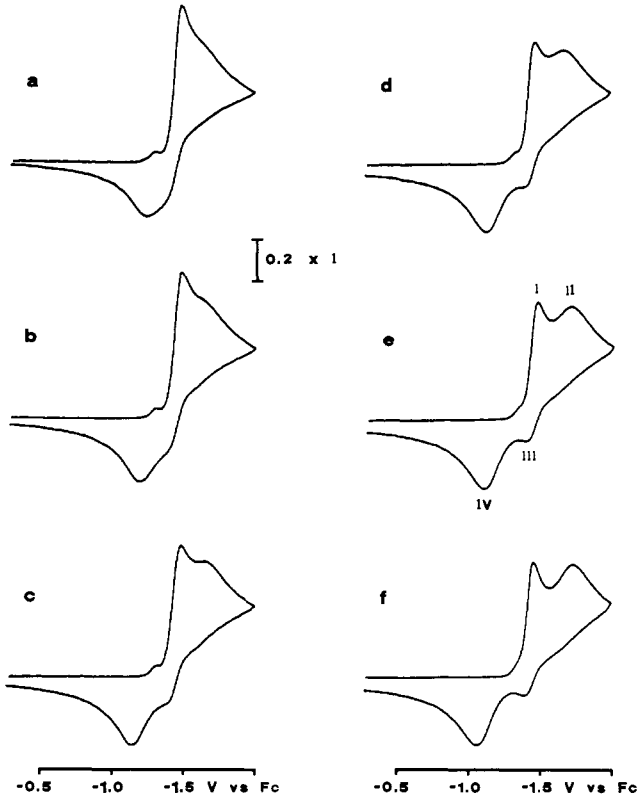

Figure 5. Faster CV scans of 1.3 mM $[(\eta^6\text{-}C_6Me_6)_2Ru][BF_4]_2$ in CH_3CN at Pt disk (d = 476 μm). Scan rates: (a) 1.0, (b) 2.0, (c) 5.0, (d) 10, (e) 20, and (f) 50 V s^{-1}. Normalized current axis, ohmic compensation 26 kΩ.

Table III. Measured Diffusion Coefficients for $(\eta^6\text{-}C_6Me_6)_2Ru^{2+}$ and $(\eta^6\text{-}C_6Me_6)(\eta^4\text{-}C_6Me_6)Ru$

compound	solvent	method	D_o (cm^2 s^{-1})
$(\eta^6\text{-}C_6Me_6)_2Ru^{2+}$, 1^{2+}	CH_2Cl_2	chronoamp	7.6×10^{-6}
$(\eta^6\text{-}C_6Me_6)_2Ru^{2+}$, 1^{2+}	CH_3CN	chronoamp	6.8×10^{-6}
$(\eta^6\text{-}C_6Me_6)_2Ru^{2+}$, 1^{2+}	CH_3CN	RDE[a]	7.6×10^{-6}
$(\eta^6\text{-}C_6Me_6)(\eta^4\text{-}C_6Me_6)Ru$, **2**	CH_3CN	RDE[a]	1.7×10^{-5}

[a] Rotating disk electrode voltammetry.

of two-electron height is observed at slow CV sweep rates in CH_3CN (Figures 3 and 4). The apparent negative shift of E°_1 with respect to E°_2 when the solvent is changed from CH_2Cl_2 to CH_3CN is rationalized on the basis that the latter more strongly solvates species of higher positive charge,[69] resulting in preferential stabilization of the dication over the monocation or neutral complex and a thermodynamically more difficult first reduction. When low v and a Hg electrode were used, deviations from Nernstian behavior were only slight (Table IIC). Thus, with v = 0.05–0.2 V s^{-1}, ΔE_p was 42 mV and $E_p - E_{p/2}$ (δE_p) was 37 mV. These data suggested a two-electron wave with closely overlapping components,[17] i.e., $\Delta E^\circ \approx 0$ V. The chemical reversibility of this wave was incomplete, with a measured i_a/i_c value of 0.56 at v = 0.05 V s^{-1}. The instability of the monocation intermediate was also suggested by (i) a cathodic product peak at −2.3 V observed when slow sweeps were extended to more negative potential (Figure 12), (ii) double potential step chronoamperometry,[64] and (iii) bulk coulometry at 243 K (1.3F; exclusive product waves at E_{pc} = −2.3 V, E_{pa} = −0.4 and +0.1 V).

At higher sweep rates (Figures 5 and 6) the cathodic branch broadens and finally splits into two waves above about v = 5 V s^{-1}. Referring to Figure 5e, peaks I and III are the cathodic and anodic features of the Ru(II)/Ru(I) couple, $1^{2+}/1^+$ (eq 3). Peak II arises from $1^+ + e^- \rightarrow$ **2** [Ru(I)/Ru(0), forward direction of eq 4]. Peak IV is the anodic reaction for oxidation of **2** and

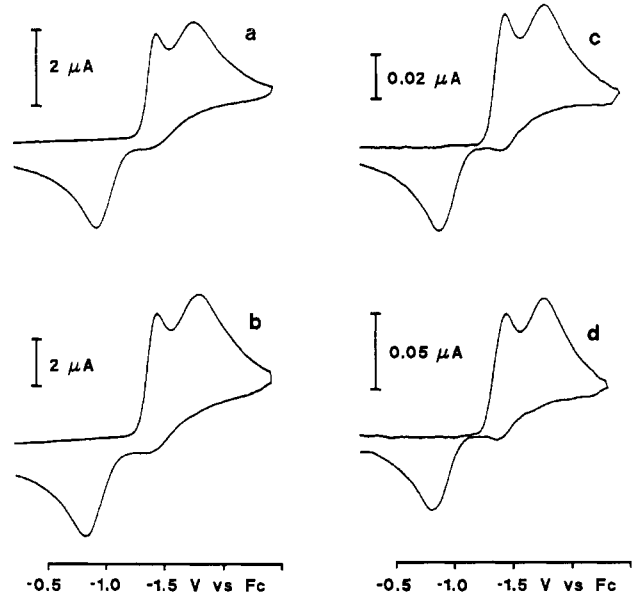

Figure 6. Very fast CV scans of 1.0 mM $[(\eta^6\text{-}C_6Me_6)_2Ru][BF_4]_2$ in CH_3CN at Pt disk. Sweep rates: (a) 600, and (b) 1800 V s^{-1}, at d = 250 μm disk and (c) 6000 and (d) 11 000 V s^{-1}, at d = 10 μm disk.

comprises the two-electron chemistry of eq 9. The one-electron reverse reaction of eq 4, involving **2** → $1^+ + e^-$, does not come into play in wave IV owing to the thermodynamic instability of 1^+ at this potential (transient 1^+ immediately oxidizes to 1^{2+} in wave IV). The very small contribution at wave III arises from 1^+ present through incomplete electrolysis in the cathodic scan.

$$\mathbf{2} \rightleftharpoons 1^{2+} + 2e^- \qquad (9)$$

With further increases in v, there was improved resolution of the two cathodic waves as well as the two anodic components. Peaks I–IV persisted as the only waves to scan rates in excess of 10 000 V s^{-1} (Figure 6). Restriction of the potential scan range

(69) Case, B. In *Reactions of Molecules at Electrodes*; Hush, N. S., Ed.; Wiley-Interscience: London, 1971; p 113ff.

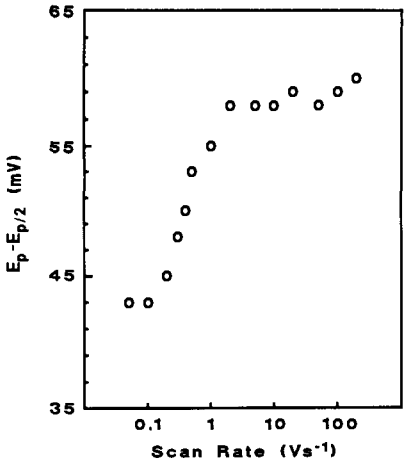

Figure 7. Peak widths, δE_p ($\equiv E_p - E_{p/2}$) for the first cathodic wave of $(\eta^6\text{-}C_6Me_6)_2Ru^{2+}$ in CH_3CN as function of sweep rate.

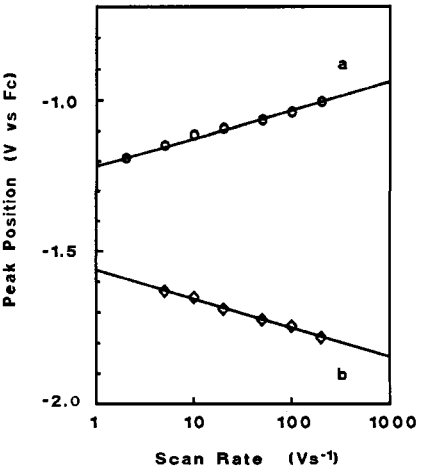

Figure 8. Potentials of (a) anodic and (b) cathodic peaks for the Ru(I)/Ru(0) couple in CH_3CN at Pt disk (d = 476 μm) as function of scan rate, peaks IV and II, respectively.

(Figure B, supplementary material) yielded values of ΔE_p for the first, Ru(II/I), reduction.

Slight differences in voltammograms were noted with Pt electrodes subjected to different pretreatments. Polished disk electrodes showed the greatest degree of reproducibility, with ΔE_p values of the $(C_6Me_6)_2Ru^{2+/+}$ [Ru(II/I)] couple and the cathodic peak width for $(C_6Me_6)_2Ru^{+/0}$ [Ru(I/0)] differing by less than 10% in replications months apart. However, bead electrodes pretreated with an HNO_3 reflux/Fe^{2+} soak cycle performed poorly, with ΔE_p values varying by as much as 50% on successive days. Consequently, only data recorded at Pt disk electrodes were examined for quantitation and kinetic information.

At the concentrations normally employed in CV studies (above 10^{-4} M) it might be anticipated that the disproportionation equilibrium (DISP) of eq 10 would influence the reaction

$$2\mathbf{1}^{2+} \underset{k_{comp}}{\overset{k_{disp}}{\rightleftharpoons}} \mathbf{1}^{2+} + 2 \quad K_{DISP} = [\mathbf{1}^{2+}][\mathbf{2}]/[\mathbf{1}^{+}]^2 \qquad (10)$$

mechanism.[14,15] Indeed, this homogeneous reaction profoundly influences both wave shapes and the possibility of viewing wave splitting. When the DISP reaction is fast (slow scan limit), the height of peak I is greatly increased compared to peak II, since much of the one-electron intermediate ($\mathbf{1}^+$) returned to reducible $\mathbf{1}^{2+}$ through eq 10 is further reduced at the potential of peak I. A number of theoretically generated voltammograms demonstrating the effects of scan rate and disproportionation rates on wave splitting are presented in Figure A of supplementary material and in ref 64.

B. Quantitative Aspects: Diagnostic Criteria. The shapes and peak positions of the cathodic features were compared to theoretical expectations for various electrode mechanisms, according to standard electrochemical practice.[70] Taken together, these comparisons were only consistent with an $E_{rev}E_{qrev}$ mechanism. Most informative were how the values of $\delta E_p (= E_p - E_{p/2})$ and E_{pc} changed with scan rate.

Peak Widths. The parameter δE_p is sensitive to heterogeneous charge-transfer kinetics, and, in an EE mechanism, the value of $E^\circ_2 - E^\circ_1$. If $E^\circ_2 \gg E^\circ_1$ and both change transfers are Nernstian, δE_p is 28.5 mV. If $E^\circ_2 \approx E^\circ_1$, its value is ca. 42 mV, and if $E^\circ_2 \ll E^\circ_1$, two one-electron waves are present, each with δE_p = 57 mV.[11] Our experimental data for $(C_6Me_6)_2Ru^{2+/+/0}$ in CH_3CN show that the width of the *first* cathodic wave increases from δE_p = 43 mV to δE_p = 60 mV (Figure 7) as the scan rate is increased from 0.05 to 200 V s^{-1}. The Ru(II/I) wave (eq 3) therefore is characteristic of a fast one-electron transfer at high sweep rates. The $E_{1/2}$ value for the Ru(II/I) couple (−1.43 V) was constant (±6 mV) over this range. The value of δE_p for the second wave (II), not precisely measurable by inspection owing to incomplete resolution (Figures 5 and 6), was in the range expected for an irreversible wave ($\delta E_p = 48/\alpha n$ mV).[71,72]

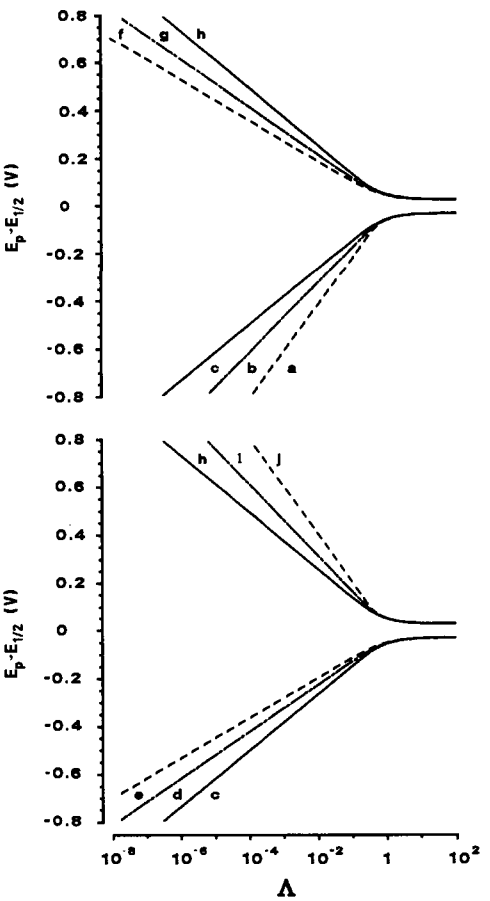

Figure 9. Calculated shift of peak potentials from $E_{1/2}$ for cathodic (a–e) and anodic (f–j) features of CV traces as function of the dimensionless kinetic parameter Λ, and α_o. α_o = (a, f) 0.3, (b, g) 0.4, (c, h) 0.5, (d, i) 0.6, (e, j) 0.7 (T = 298 K, n = 1, $D_O = D_R$).

Peak Potential Shifts with Scan Rate. At scan rates sufficiently high to produce wave splitting, the potential of the first cathodic wave (I, Figure 5e) as well as that of the coupled anodic wave (III), was essentially independent of scan rate. Because no rate limitations (peak shifts) were observed for this Ru(II/I) couple up to ca. 100 V s^{-1}, its k_{s1} value was assigned a lower limit of 2 cm s^{-1}. Peaks II and IV, however, shifted linearly with log scan

(70) Although inherent to electrodic analysis, this approach was popularized after the following: Nicholson, R. S.; Shain, I. *Anal. Chem.* **1964**, *36*, 706. Collected summaries may be found: (a) Brown, E. R.; Sandifer, J. R. In *Physical Methods of Chemistry*; Rossiter, B. W., Hamilton, J. F., Eds.; John Wiley and Sons: New York, 1986; Vol. II, Chapter 4. (b) Macdonald, D. D. *Transient Techniques in Electrochemistry*; Plenum Press: New York, 1977. (c) Galus, Z. *Fundamentals of Electrochemical Analysis*; Horwood Publ.: Chichester, 1976. (d) Reference 7.

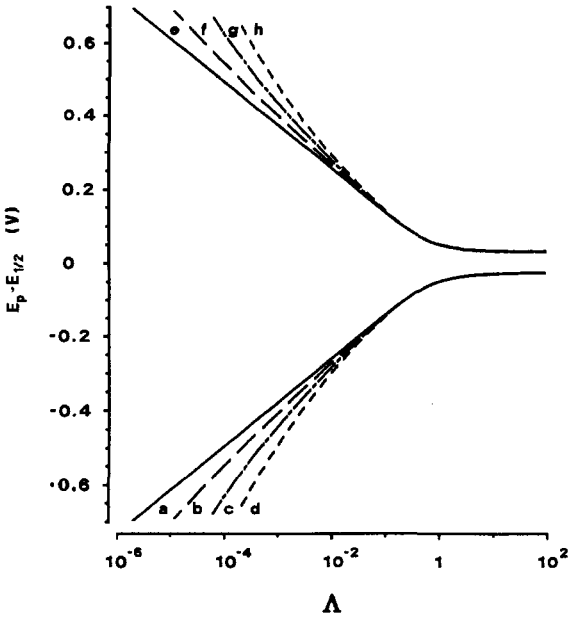

Figure 10. Calculated shift of peak potentials from $E_{1/2}$ for cathodic (a–d) and anodic (e–h) features of CV traces as function of dimensionless kinetic parameter Λ for $\alpha_o = 0.50$, with potential dependencies for α, $d\alpha/dE$, of (a, e) 0, (b, f) 0.10, (c, g) 0.20, (d, h) 0.30 (T = 298 K, n = 1, $D_O = D_R$).

rate (Figure 8). The theoretical slope of E_p vs log v for a reduction limited by slow charge transfer is $-29.6/\alpha n$ mV.[71,72] Although we have not been able to find explicit treatments of the expected shift for the coupled anodic wave, a value of $29.6/(1-\alpha)n$ mV per decade in v seemed logical. This reasoning was confirmed by digital simulations (Figure 9).[73]

The measured peak shifts were equal and opposite, −92 and +92 mV per decade, respectively, for the cathodic and anodic processes of waves II and IV. The occurrence of equal slopes of opposite sign is *only* consistent with $\alpha = 0.50$. However, the absolute value of the cathodic slope suggests an α value of 0.7, whereas that of the anodic slope predicts $\alpha = 0.3$. Given this inconsistency, it was apparent that another factor influenced the peak potentials, and it was not surprising that k_{s2} values calculated simply from ΔE_p values for peaks II and IV[74] varied greatly over the scan rate range of 5–200 V s^{-1}.[75]

These systematic deviations from Butler–Volmer kinetics[76] are explained by a potential dependence of the transfer coefficient. Marcus predicted that this dependence takes the form of eq 11,[77] wherein α_o is the value of the transfer coefficient

$$\alpha = \alpha_o + (d\alpha/dE)(E_{app} - E^\circ) \qquad (11)$$

at the standard potential E°, with α values becoming smaller at potentials negative of E° and larger at more positive potentials. There is considerable controversy over reports which have claimed to verify this aspect of Marcus theory.[78] However, our analysis

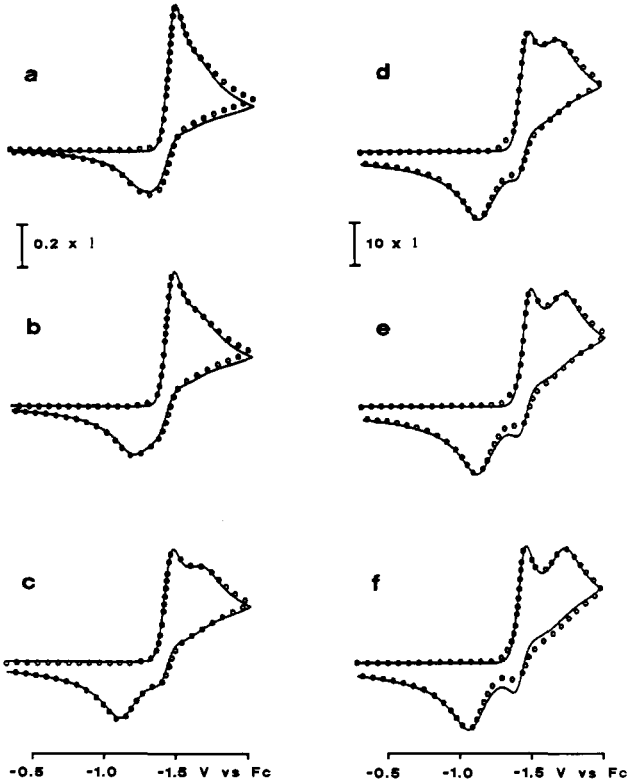

Figure 11. Digital simulations compared to experimental CV scans (circles). Experimental conditions, 1.0 mM $[(\eta^6\text{-}C_6Me_6)_2Ru][BF_4]_2$ in CH_3CN, 0.21 mm disk, ohmic compensation 2.0 kΩ. Scan rates: (a) 0.40, (b) 1.0, and (c) 5.0 V s^{-1}. Scans (d–f) used 476 μm Pt disk, 26 kΩ compensation for sweep rates: (d) 10, (e) 20, and (f) 50 V s^{-1}. Exact simulation parameters are given in supplementary material, and average values are given in Table IV.

appears to require a potential-dependent α value.

Since low $d\alpha/dE$ values are predicted for redox systems with large reorganizational barriers,[77] apparent changes in α are difficult to detect for slow charge-transfer systems *unless* the voltammetric peaks are well displaced from E°. Since the $(C_6Me_6)_2Ru^{+/0}$ couple fulfills this requirement, it was of interest to see if the anomalous peak shifts could be quantitatively explained by a transfer coefficient given by eq 11.

Computations were made of peak shifts versus the dimensionless kinetic variable Λ from simulated voltammograms assuming a

$$\Lambda = \Psi\pi^{1/2} = k_s[D_O^{(1-\alpha)}D_R^{\alpha}(nFv/RT)]^{-1/2} \qquad (12)$$

potential-dependent transfer coefficient. Results are shown in Figure 10 for various $d\alpha/dE$ values. Note that for $\alpha_o = 0.5$ in the limit of slow charge transfer or high scan rates ($\Lambda < 0.1$), *equal and opposite* slopes of peak shifts are predicted, with absolute values *larger* than those predicted for a potential-*in*dependent α. The experimental slopes for $(C_6Me_6)_2Ru^{+/0}$ (±92 mV) matched well with predictions for $d\alpha/dE$ of ca. 0.2 V^{-1} (curves c and g, Figure 10), with k_{s2} estimated as 5×10^{-4} cm s^{-1} (see ref 75).

C. Quantitative Aspects: Digital Simulations. Section B emphasized agreement between theory and experiment at certain points in the voltammetric curves, namely the half-peak and peak positions. A more global analysis was desired, so digital simulations of the entire CV response were performed. The following reactions were included in the simulations:

$$1^{2+} + e^- \rightleftharpoons 1^+ \qquad E^\circ_1,\ \alpha_1,\ k_{s1} \qquad (13)$$

$$1^+ \rightarrow Z \qquad \text{rate} = k_c \qquad (14)$$

$$1^+ + e^- \rightleftharpoons 2 \qquad E^\circ_2,\ \alpha_2,\ k_{s2} \qquad (15)$$

$$21^+ \rightleftharpoons 1^{2+} + 2 \qquad \text{rate (f)} = k_{disp};\ \text{rate (b)} = k_{comp} \qquad (16)$$

The starting points for the simulations were the facts gathered from the previous sections, namely that (a) $E^\circ_2 - E^\circ_1$ was ca. 0

(71) Nicholson, R. S.; Shain, I. *Anal. Chem.* **1964**, *36*, 706.
(72) Matsuda, H.; Ayabe, Y. *Z. Electrochem.* **1955**, *59*, 494.
(73) The complimentarity of E_{pc} and E_{pa} shifts (through α and 1-α terms) is analogous to theory and observation for cathodic and anodic Tafel slopes, see: e.g., Delahay, P. *New Instrumental Methods in Electrochemistry*, Interscience: New York, 1954; pp 40–41. This concept is also implicit in the treatments of Ryan (ref 14) and Hinkelmann and Heinze (ref 15).
(74) Nicholson, R. S. *Anal. Chem.* **1965**, *37*, 1351.
(75) Apparent values of k_{s2} decreased from 5.3×10^{-4} to 2.0×10^{-4} cm s^{-1} as v increased from 5 to 200 V s^{-1} when measured from the ΔE_p.
(76) Bockris, J. O'M.; Reddy, A. K. N. *Modern Electrochemistry*; Plenum Publishers: New York, 1970; Vol. 2, p 880.
(77) (a) Marcus, R. A. *J. Phys. Chem.* **1963**, *67*, 853. (b) Marcus, R. A. *J. Chem. Phys.* **1965**, *43*, 679. (c) Cannon, R. D. *Electron Transfer Reactions*; Butterworths: London, 1980; p 205ff.
(78) (a) Saveant, J. M.; Tessier, D. *J. Electroanal. Chem.* **1975**, *65*, 57. (b) Weaver, M. J.; Anson, F. C. *J. Phys. Chem.* **1976**, *80*, 1976. (c) Corrigan, D. A.; Evans, D. H. *J. Electroanal. Chem.* **1987**, *233*, 161. (d) O'Dea, J. J.; Osteryoung, J.; Osteryoung, R. A. *J. Phys. Chem.* **1983**, *87*, 3911. Nine additional references are in supplementary material.

Table IV. Average Best-Fit Results for Digital Simulation Analysis[a]

E°_1 (V)	k_{s1} (cm s^{-1})	E°_2 (V)	k_{s2} (cm s^{-1})	$\alpha_{o,2}$	$d\alpha_2/dE$ (V^{-1})	k_c (s^{-1})	k_{disp} (M^{-1} s^{-1})
−1.43 (1)	>2.0	−1.40 (1)	4.5 (9) × 10^{-4}	0.50 (2)	0.22 (4)	1.0 (1)	6.3 (8) × 10^4

[a] $(C_6Me_6)_2Ru^{2+/+/0}$ in CH_3CN/Bu_4NPF_6, ambient temperature, potentials vs Fc/Fc^+. Values in parentheses are the estimated errors in the last digit.

V, (b) $k_{s2} \ll k_{s1}$, $\alpha_2 = 0.5 + 0.2\,(E_{appl} - E^\circ)$, and (c) k_c ca. 1.0 s^{-1}. The value of α_1 had no effect on wave shapes as expected for a fast charge-transfer reaction and was set arbitrarily at $\alpha_1 = 0.5$.[79]

The fits were accomplished by visually matching theoretical and experimental curves. Error limits were estimated for each parameter, with respect to the set of best fit, by individually increasing or decreasing the variable until the voltammetric peaks deviated more than ±10 mV on the potential axis or by more than ±2% on the current axis. If the kinetic regime was such that values could not be confidently assigned to some parameters (e.g., k_{s1}), a limiting value is reported.

Figure 11 shows a representative series of fits obtained for CV's recorded in CH_3CN/0.1 M Bu_4NPF_6 at Pt disk electrodes. A table giving a complete list of the parameters of 15 simulations of experiments at concentrations of 0.5–1.3 mM and sweep rates of 0.4–100 V s^{-1} is available as supplementary material. Table IV gives the average of these parameters. Because no deviation from a Nernstian ΔE_p was observed for the first wave when positive feedback was used, up to $v = 100$ V s^{-1}, Ru(II/I) was assigned a value of $k_{s1} > 2$ cm s^{-1} in the simulations.

The second reduction had $E^\circ_2 = -1.40$ V ± 0.01 V, whereas the first reduction was 30 mV more *negative*, $E^\circ_1 = -1.43$ V ± 0.01 V. Average values of $k_{s2} = (4.5 \pm 0.9) \times 10^{-4}$ cm s^{-1} and $\alpha_{o,2} = 0.50 \pm 0.02$ were obtained. As anticipated from peak potential measurements, the latter was found to vary with potential as $d\alpha/dE = 0.22 \pm 0.04$ V^{-1}. It was found that the potential-dependent α value accounted not only for the magnitude of the peak shifts with v but also the large breadth of both peaks II ($\mathbf{1}^+ \rightarrow \mathbf{2}$) and IV ($\mathbf{2} \rightarrow \mathbf{1}^{2+}$). Simulations using a constant α_2 matched poorly at high sweep rates, where peaks II and IV were well-separated from E°_2.

It was also apparent that the rates of the disproportionation/comproportionation reactions (eq 16) were considerably less than diffusion limited. Lower computational values of k_{disp} and k_{comp} led to conspicuous enhancement of peak II at the expense of peak I. The effect of k_{disp} on the anodic portions was to decrease the relative contribution of peak III with a slower homogeneous reaction. The average value of k_{disp} obtained from the simulations, $(6.3 \pm 0.8) \times 10^4$ M^{-1} s^{-1}, was used with K_{DISP} for eq 16 (2 ± 1, set by $E^\circ_2 - E^\circ_1$) to calculate $k_{comp} = (2.9 \pm 0.4) \times 10^4$ M^{-1} s^{-1}.

Finally, mismatches of current heights in the anodic region led us to question the role of the relative diffusion coefficients (D) of $\mathbf{1}^{2+}$, $\mathbf{1}^+$, and **2** on the observed traces. Theoretical simulations (Figure C, supplementary material) bear out that the ratio $D(\mathbf{1}^{2+})/D(\mathbf{2})$ exerts an influence, particularly on wave III, in the presence of a DISP reaction. If this ratio is less than unity, **2** diffuses through a larger volume of solution and reacts less efficiently with $\mathbf{1}^{2+}$, diminishing the amount of $\mathbf{1}^+$ formed through eq 10 and *lowering* the height of the $\mathbf{1}^+/\mathbf{2}$ wave (wave III). Conversely, if $D(\mathbf{1}^{2+})/D(\mathbf{2}) > 1$, **2** remains close to the electrode, helping to drive the reverse reaction of eq 10, and wave III is *enhanced* at the expense of wave IV. The former was necessary to fit the observed anodic currents for the Ru system. Optimum agreement was found with $D(\mathbf{1}^{2+})/D(\mathbf{2}) = 0.38$.

An independent verification of the conclusion that $D(\mathbf{1}^{2+}) < D(\mathbf{2})$ was obtained through voltammetry at a rotating Pt disk electrode. Concentrations of about 0.30 mM were employed in separate experiments with CH_3CN solutions of the dication and of the neutral complex. The experiments were carried out inside a drybox owing to the air sensitivity of $(\eta^6\text{-}C_6Me_6)(\eta^4\text{-}C_6Me_6)Ru$, **2**. Linear Levich plots[80] were obtained over the rotation rate range of 500–3000 rpm with diffusion coefficients calculated as 1.7×10^{-5} cm^2 s^{-1} and 7.6×10^{-6} cm^2 s^{-1} for **2** and $\mathbf{1}^{2+}$, respectively. The experimental ratio of 0.45 for $D(\mathbf{1}^{2+}/\mathbf{2})$ is close to that (0.38) suggested by the digital simulations of $\mathbf{1}^{2+}/\mathbf{1}^+/\mathbf{2}$.

(79) A value of approximately 0.5 for α is common for fast (uncomplicated) electron-transfer reactions.

Discussion

Reasonably exhaustive calculations involving both heterogeneous and homogeneous aspects of the electron-transfer properties of $\mathbf{1}^{2+}$, $\mathbf{1}^+$, and **2** were necessary to account for the waveshapes observed for the reduction of $(\eta^6\text{-}C_6Me_6)_2Ru^{2+}$ in CH_3CN. The variables involved in this process included the E°, k_s, and α values for each redox couple, the decomposition rate constant of $\mathbf{1}^+$ (k_c), the ratio of diffusion coefficients for $\mathbf{1}^{2+}$ and **2**, the rates of the homogeneous DISP reaction, and the potential dependence of the transfer coefficient α. Fortunately, there are opportunities to check the final values of these parameters (Table IV) for reasonableness, given our knowledge of the chemical system under study, expectations based on theory, and literature precedents. Each parameter will be briefly considered.

(1) Thermodynamic Factor, $E^\circ_2 - E^\circ_1$ (ΔE°). It is informative to compare the values of ΔE° for $\mathbf{1}^{2+}/\mathbf{1}^+/\mathbf{2}$ in the two solvents, CH_2Cl_2 (−0.14 V) and CH_3CN (+0.03 V). In the more basic solvent, CH_3CN, a shift of +170 mV is calculated for the couple $\mathbf{1}^+/\mathbf{2}$ relative to $\mathbf{1}^{2+}/\mathbf{1}^+$. The value of this solvent-induced change in ΔE° has been measured for $(\eta^6\text{-}C_6Me_6)RhCp^{*\,2+/+/0}$ and estimated for $(\eta^6\text{-}C_6Me_6)IrCp^{*\,2+/+/0}$, two close analogues, as +120[46] and +250 mV,[25] respectively. The direction and magnitude of the solvent effect on ΔE° is, therefore, as expected.

(2) Heterogeneous Electron-Transfer Rates, k_{s1} and k_{s2}. The Ru(II/I) couple has a very fast heterogeneous charge-transfer rate. We estimate a lower limit of k_{s1} as 2 cm s^{-1} from our data, in the normal range for metal sandwich compounds undergoing minor geometric changes upon reduction.[81]

From the value of $k_{s2} = 4.5 \times 10^{-4}$ cm s^{-1} for the Ru(I/0) couple an activation free energy for electron transfer, ΔG^*, of 40 kJ/mol may be calculated assuming a value of 5×10^3 cm/s for the heterogeneous collision frequency.[82] It is useful to see if this barrier may be accounted for through Marcus–Hush rate theory.[83]

Ignoring work terms and the so-called "Frumkin correction",[84] the activation barrier is related to the inner-sphere and outer-sphere reorganization energies, λ_i and λ_o, respectively, by eq 17[85]

$$\Delta G^* = \tfrac{1}{4}(\lambda_i + \lambda_o) \qquad (17)$$

Since λ_o arises from solvent dielectric reorganization, its value is readily estimated based on results for other metal sandwich redox processes involving like-charged species. Gennett and Weaver suggest a value of $\lambda_o = 24$ kJ/mol for (+/0) metallocene couples in CH_3CN,[86] far too low to account for the observed activation barrier in Ru(I/0). It is therefore implied that in-

(80) Reference 7, p 288.
(81) Nielson, R. M.; Golvin, M. N.; McManis, G. E.; Weaver, M. J. *J. Am. Chem. Soc.* **1988**, *110*, 1745, and references therein.
(82) Hale, J. M. in ref 69, p 230ff.
(83) (a) Hush, N. S. *Z. Elekrochem.* **1957**, *61*, 734. (b) Hush, N. S. *J. Chem. Phys.* **1958**, *28*, 962. (c) Marcus, R. A. *J. Chem. Phys.* **1965**, *43*, 679. (d) Waisman, E.; Worry, G.; Marcus, R. A. *J. Electroanal. Chem.* **1977**, *82*, 9.
(84) The work required to transport the reactant from the bulk of solution to the preelectron transfer site near the electrode is often ignored because of ambiguities in electrode/reactant distances. See: discussions in refs 52c and 100 as well as Schmickler and Henderson (Schmickler, W.; Henderson, D. *Prog. Surf. Sci.* **1986**, *22*, 323).
(85) Reference 82, p 249.
(86) Reference 52c. Weaver, M. J.; Gennett, T. *Chem. Phys. Lett.* **1985**, *113*, 213.

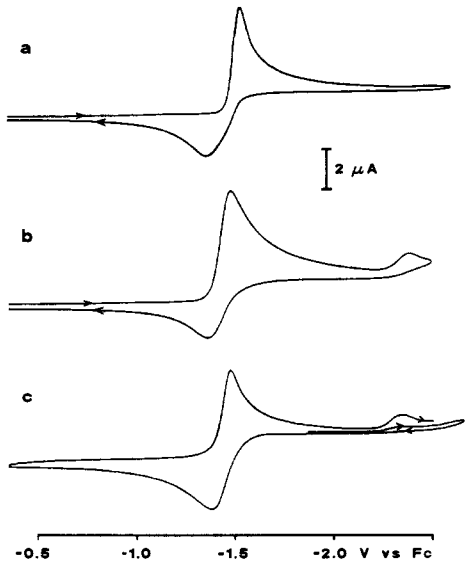

Figure 12. CV scans to more negative potentials for 0.5 mM $[(\eta^6\text{-}C_6Me_6)_2Ru^{2+}][BF_4]_2$ in CH_3CN at Pt bead at T = (a) 263 and (b) 298 K. Scan (c) is for 0.5 mM $(\eta^6\text{-}C_6Me_6)(\eta^4\text{-}C_6Me_6)Ru$ in CH_3CN at 283 K. Scan rate = 0.2 V s^{-1}.

ner-sphere (molecular geometry) changes are the major contributor to the Ru(I/0) activation barrier.

The inner-sphere (Franck–Condon) activation free energy may in principle be calculated from eq 18, in which Δa_i represents the

$$\Delta G^*_i = 0.5n\sum f_i(\tfrac{1}{2}\Delta a_i)^2 \qquad (18)$$

atomic displacements accompanying the electron-transfer reaction, and f_i are the reduced force constants of the ith chemical bonds.[87] However, although the structural data of Huttner and Lange[88] on $(\eta^6\text{-}C_6Me_6)(\eta^4\text{-}C_6Me_6)Ru$ allow evaluation of the Δa_i values, the requisite force constant data are not available.

An approach to the estimation of λ_i is based on the idea that bending of the arene requires fracture of a Ru–olefin bond. Saveant has shown that in an irreversible electron-transfer reaction, λ_i may be given approximately by the bond dissociation energy.[89] On the basis of available numbers for the enthalpy of Fe–arene bonds[90] and the expectation that arenes are bound more strongly to second-row metals,[91] we estimate a value of ca. 300 kJ/mol for an arene–Ru dissociation energy and use $^1/_3$ of this value for the cleavage energy of a single Ru to C=C arene bond (λ_i in eq 17). The resulting estimate of 31 kJ/mol for ΔG^* of eq 4 is in moderate agreement with the "experimental" value of ca. 40 kJ/mol.

The low theoretical estimate for ΔG^* may be indicative that an interfacial effect contributes to the height of the activation barrier. We have now observed a number of examples in which et reactions involving metal–arene hapticity changes are abnormally slow on Pt compared to, e.g., glassy carbon. Given the well-established affinity of Pt for olefins,[92] the interfacial interaction may involve a transient intermediate or transition state structure similar to that shown below

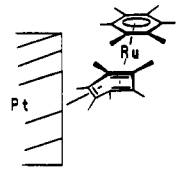

(3) Decomposition Rate of 1^+. A rate constant of 1.0 s^{-1} (assuming first-order kinetics) for the decomposition rate of the one-electron intermediate, $(C_6Me_6)_2Ru^+$, is consistent with two other electrochemical observations, namely the formation of side product(s) in bulk electrolyses, and the presence of a peak for the side-reaction product in slow CV scans taken to more negative potentials (Figure 12). Double potential step chronoamperograms also suggested follow-up reactions over the same time scale.[64]

(4) Diffusion Coefficient Difference for 1^{2+} and 2. We found it surprising that simulations suggested such a large deviation from unity for the diffusion coefficient ratio $D(\mathbf{1}^{2+})/D(\mathbf{2})$, since it is usually assumed that D(red) = D(ox) for a redox couple.[93] However, independent measure of the diffusion coefficients for $\mathbf{1}^{2+}$ and **2** with the rotating disk electrode (ratio = 0.45) lends credence to this observation.

(5) Disproportionation Rate Constants, k_{disp} and k_{comp}. Our results require rates for the DISP reaction (eq 16) of ca. 10^4–10^5 M^{-1} s^{-1}, approximately four orders of magnitude below a diffusion-controlled[94] rate, but consistent with theory for systems undergoing electron transfer concomitant with significant structural change.[77,95] Consultation of papers and reviews[96] show that these values are not unusually low for structurally-variant outer-sphere electron-exchange reactions.

A recent study by Nielson and Weaver[48] allows a prediction of k_{disp} for $(C_6Me_6)_2Ru^+$. These authors used NMR line-broadening techniques to measure the self-exchange rates for $(\eta^6\text{-}C_6Me_6)RhCp^{*2+/+}$ (eq 19) and $(\eta^6\text{-}C_6Me_6)RhCp^{*+}/(\eta^4\text{-}C_6Me_6)RhCp^*$ (eq 20).

$$(\eta^6\text{-}C_6Me_6)RhCp^{*2+} + (\eta^6\text{-}C_6Me_6)RhCp^{*+} \rightleftharpoons (\eta^6\text{-}C_6Me_6)RhCp^{*+} + (\eta^6\text{-}C_6Me_6)RhCp^{*2+} \qquad (19)$$

$$(\eta^6\text{-}C_6Me_6)RhCp^{*+} + (\eta^4\text{-}C_6Me_6)RhCp^* \rightleftharpoons (\eta^4\text{-}C_6Me_6)RhCp^* + (\eta^6\text{-}C_6Me_6)RhCp^{*+} \qquad (20)$$

The rate constants measured in acetone for eqs 19 and 20, were 3.3×10^5 and 8.3×10^2 M^{-1} s^{-1}, respectively. We expect similar values for the 2+/+ and +/0 couples in $(C_6Me_6)_2Ru^{2+/+/0}$, since the two sets of complexes have the same size and charge and undergo similar geometric changes. These rate constants (k_{SE}) may be used with the Marcus cross-reaction equation (eq 21) to predict k_{disp}[97] for $(C_6Me_6)_2Ru^+$ (eqs 10 or 16) as 4×10^4 M^{-1} s^{-1}, consistent with the value of 6.3×10^4 M^{-1} s^{-1} found through simulation fits.[98]

$$k_{disp}^2 = k_{SE(2+/+)}k_{SE(+/0)}K_{DISP} \qquad (21)$$

(87) Sutin, N. In *Progress in Inorganic Chemistry*; Lippard, S. J., Ed.; John Wiley and Sons: New York, 1983; Vol. 30, p 441, and references therein.

(88) Huttner, G.; Lange, S. *Acta Crystallogr.* **1972**, *B28*, 2049.

(89) Saveant, J.-M. *J. Am. Chem. Soc.* **1987**, *109*, 6788.

(90) A bond dissociation energy for benzene–Fe^+ of 230–240 kJ/mol is reported: (a) Hettich, R. L.; Jackson, T. C.; Stanko, E. M.; Freiser, B. S. *J. Am. Chem. Soc.* **1986**, *108*, 5086. (b) Jacobson, D. B.; Freiser, B. S. *J. Am. Chem. Soc.* **1984**, *106*, 3900.

(91) The arene dissociation energy is ca. 50–80 kJ/mol higher for (arene)Mo than for (arene)Cr: (a) Connor, J. A. *Top. Curr. Chem.* **1977**, *71*, 71. (b) Skinner, H. A.; Connor, J. A. *Pure Appl. Chem.* **1985**, *57*, 79.

(92) Lane, R. F.; Hubbard, A. T. *J. Phys. Chem.* **1973**, *77*, 1401, 1411.

(93) A recent theoretical paper addresses the general significance of unequal diffusion coefficients of homogeneous reactants in electrochemistry: Andrieux, C. P.; Hapiot, P.; Saveant, J. M. *J. Electroanal. Chem.* **1984**, *172*, 49. See, also: DeJong, H. G.; Van Lauwen, H. P.; Holub, K. *J. Electroanal. Chem.* **1987**, *234*, 1, 17; *235*, 1. Ruzic, I.; Smith, D. E.; Feldberg, S. W. *J. Electroanal. Chem.* **1974**, *52*, 157. Evans, D. H. *J. Electroanal. Chem.* **1989**, *258*, 451.

(94) Inorganic systems: ref 77c, p 100ff. Organic systems: Kojima, H.; Bard, A. J. *J. Am. Chem. Soc.* **1975**, *97*, 6317.

(95) Weaver, M. J.; Hupp, J. T. In *Mechanistic Aspects of Inorganic Reactions*; Rorabacher, D. B., Endicott, J. F., Ed.; ACS Symposium Series; American Chemical Society: Washington, DC, 1982; Vol. 198, p 181.

(96) (a) Taube, H. *Comments Inorg. Chem.* **1981**, *1*, 17. (b) Endicott, J. F.; Kumar, K.; Ramasami, T.; Rotzinger, F. P. In *Progress in Inorganic Chemistry*; Lippard, S. J., Ed.; Wiley: New York, 1983; Vol. 30, p 141. Four additional references are in supplementary material.

(97) Marcus, R. A. *Ann. Rev. Phys. Chem.* **1964**, *15*, 155.

(98) It should be noted that eq 21 refers to outer-sphere self-exchange reactions and that it may not be applicable where conformational changes are sequential with, rather than concerted with, electron transfer. See: ref 58a as well as Lee and Anson (Lee, C.-W.; Anson, F. C. *Inorg. Chem.* **1984**, *23*, 837).

(6) Potential-Dependent α Value. The potential dependence of α is predicted by Marcus[99,100] to be related to the reorganizational energy λ by eq 22.

$$d\alpha/dE = nF/4\lambda; \qquad \lambda = \lambda_i + \lambda_o \tag{22}$$

Using the "experimental" value of λ = 160 kJ/mol, the potential-dependent coefficient $d\alpha/dE$ is predicted to be 0.15 V^{-1}. The value predicted from the theoretical λ calculation of section (2) above is 0.19 V^{-1} (λ = 124 kJ/mol). The measured value of $d\alpha/dE = 0.22 \pm 0.04$ V^{-1} is therefore in a range predicted both from Marcus theory and from theoretical models of reorganization energies.

Conclusions and Limitations

All CV data for $(C_6Me_6)_2Ru^{2+/+/0}$ in CH_3CN is quantitatively explained by the reactions of eqs 13–16, which essentially describe an EE DISP mechanism (eq 14 is a decomposition side reaction which is unimportant at short experiment times), and by the parameters in Table IV. Other possible mechanisms involving ECE- or EEC-type processes do not appear to account for the breadths and potential shifts with v of peaks II and IV. However, as with all mechanistic studies,[101] our data do not *prove* the $E_{rev}E_{qrev}$ formulation; rather, they demonstrate that such a mechanism gives an adequate account of experimental results within the time frame of the investigation (roughly 10 s > t > 10 μs). An important corollary of this finding is that the η^6/η^4 hapticity change must occur in *less than 10 μs before or after formation of the transition state* for the Ru(I/0) et process.

The wave splitting observed for the $(C_6Me_6)_2Ru^{2+/+/0}$ couples in CH_3CN suggests that kinetic discrimination of elementary et steps may be achieved for other multielectron systems. Three parameters will largely dictate the conditions under which wave splitting can be observed. These parameters are (1) the separation of the formal one-electron potentials (ΔE°), (2) the relative rates of the two interfacial electron transfers, and (3) the participation of solution electron transfer (SET)[102] reactions. The present work has demonstrated that a small separation in formal potentials coupled with a low ratio of k_{s2}/k_{s1} produces a favorable set of conditions for viewing this phenomenon. However, participation of SET reactions can preclude wave splitting if the rates of the homogeneous reactions approach the diffusion limit. Clearly, the lack of experimental control over these SET reactions makes their participation a most significant factor in the kinetic discrimination scheme. If the SET reactions are slow, the present work demonstrates that the remaining factors, namely ΔE° and k_s values, may be manipulated in some cases to obtain conditions favorable to observe wave splitting.

The importance of fast conformational changes coupled to electron transfer is receiving increased recognition.[103] The possibility of et intermediates of altered geometry with lifetimes long compared to the et reaction has long been recognized but seldom explicitly treated in the homogeneous et literature,[104] perhaps because optical spectra are not often diagnostic of subtle conformational and isomeric changes in metal–ligand complexes. There is often, however, sensitivity of E° potentials to conformational changes, so that electrochemistry has provided considerable information on sequences of electron transfer and structural changes. In at least one recent study,[58a] an electrochemical demonstration of a square scheme mechanism (with conformational intermediates) has been able to rationalize apparently contradictory homogeneous et rate data. Advances in ultramicroelectrode technology[105] promise to further lower the effective time scale of electrochemical observations and broaden the overlap between homogeneous and heterogeneous electron-transfer studies.

Acknowledgment. This work was supported by the National Science Foundation (CHE 86-03974). We thank V. Boekelheide for a sample of **2** and acknowledge helpful discussions with D. H. Evans and J. Heinze. W.E.G. also thanks M. Wightman and J. Howell for help in constructing microelectrodes during a visit to Indiana University.

Supplementary Material Available: Simulation parameters for CV scans (a)–(f) of Figure 11, Figures A and B showing results of digital simulations for an EE DISP mechanism as a function of scan rate (A) and with unequal diffusion coefficients for $\mathbf{1}^{2+}$ and **2** (B), Figure C showing scans of the Ru(II)/Ru(I) wave alone in CH_3CN, and an expanded reference set (16 pages). Ordering information is given on any current masthead page.

(99) Marcus, R. A. *J. Chem. Phys.* **1956**, *24*, 966. Equivalent predictions have arisen from other theoretical treatments, see leading references: Corrigan, D. A.; Evans, D. H. *J. Electroanal. Chem.* **1980**, *106*, 287.

(100) Equation 11 employs a definition of α as based on Butler–Volmer kinetics rather than Tafel slopes. A factor of 2 is involved, see: Weaver, M. J.; Anson, F. C. *J. Phys. Chem.* **1976**, *80*, 1861. Bonnaterre, R.; Cauquis, G. *J. Electroanal. Chem.* **1972**, *35*, 287.

(101) Bunnett, J. F. In *Techniques of Chemistry*; Bernasconi, C. F., Ed.; John Wiley and Sons: New York, 1986; Vol. I, Part I, Chapter IV.

(102) For a general review of the importance of SET reactions in electrochemical mechanisms, see: Evans, D. H. *Chem. Rev.* **1990**, *90*, 739.

(103) (a) Hoffman, B. M.; Ratner, M. A. *J. Am. Chem. Soc.* **1987**, *109*, 6237. (b) Nocek, J. M.; Liang, N.; Wallin, S. A.; Mauk, A. G.; Hoffman, B. M. *J. Am. Chem. Soc.* **1990**, *112*, 1623. (c) Yuan, X.; Sun, S.; Hawkridge, F. M.; Chlebowski, J. F.; Taniguchi, I. *J. Am. Chem. Soc.* **1990**, *112*, 5380.

(104) Reynolds, W.; Lumry, R. *Mechanisms of Electron Transfer*; Ronald Press: 1966; p 7 and references therein.

(105) (a) Fleischmann, M.; Pons, S.; Rolison, D. R.; Schmidt, P. P. *Ultramicroelectrodes*; Datatech Systems, Inc.: Morganton, NC, 1987. (b) Wightman, R. M.; Wipf, D. O. In *Electroanalytical Chemistry*; Bard, A. J., Ed.; Marcel Dekker: New York, 1989; Vol. 15, p 267. (c) Robinson, J. In *Comprehensive Chemical Kinetics*; Compton, R. G., Ed.; Elsevier: Amsterdam, 1989; Vol. 29, Chapter 5. (d) *Microelectrodes: Theory and Applications*; Montenegro, M. I., Queiros, M. A., Daschbach, J. L., Eds.; NATO ASI Series E; Kluwer Academic Publishers: Dordrecht, 1991; Vol. 197.